Scientia Iranica B (2011) 18 (6), 1313–1320

Sharif University of Technology
Scientia Iranica
Transactions B: Mechanical Engineering
www.sciencedirect.com

Research note

Vibration of functionally graded cylindrical shells with ring support

G.H. Rahimi [a,*], **R. Ansari** [b], **M. Hemmatnezhad** [a]

[a] *Department of Mechanical Engineering, Tarbiat Modares University, Tehran, P.O. Box 14115-143, Iran*
[b] *Department of Mechanical Engineering, University of Guilan, Rasht, P.O. Box 3756, Iran*

Received 21 December 2010; revised 11 September 2011; accepted 5 November 2011

KEYWORDS
Vibration;
FGM cylindrical shells;
Sanders' shell theory;
Ritz method;
Boundary conditions.

Abstract In this paper, the vibrational behavior of functionally graded cylindrical shells with intermediate ring supports is studied. Theoretical formulation is established based on Sanders' thin shell theory. The governing equations of motion are derived, using an energy functional and by applying the Ritz method. Using an appropriate set of displacement functions, the energy equations lead to an eigenvalue problem whose roots are the natural frequencies of vibration. Material properties are assumed to be graded in the thickness direction, according to the power-law volume fraction function. A functionally graded cylindrical shell, made up of a mixture of ceramic and metal, is considered. The influence of some commonly used boundary conditions and the effect of changes in shell geometrical parameters and variations in ring support position on vibration characteristics are studied. The results obtained for a number of particular cases show good agreement with those available in the open literature.

1. Introduction

Functionally Graded Materials (FGMs) have received considerable attention in many engineering applications, since they were first introduced in 1984 in Japan [1,2]. Covering a wide spectrum of functional operation principles and addressing a large variety of application fields, FGMs have been under world-wide development during recent years. They are now developed for general use as structural components in extremely high temperature environments, such as rocket engine components, space plan bodies, nuclear reactor components, engine components, turbine blades, hip implants and other engineering and technological applications. A detailed discussion on their design, processing and application can be found in [3]. FGMs are also promising candidates for future intelligent composites [4]. They are usually composed of two materials whose volume fractions vary smoothly and continuously from one surface to another. This leads to a continuous variation in mechanical properties. The best known FGM is compositionally graded from ceramic to metal, to incorporate the heat, wear and oxidation resistance of ceramics with the toughness, strength, machinability and bending capability of metals. With the ever increasing usage of these materials, it is important to understand the vibrating behavior of FGM cylindrical shells, which have a vast range of applications in engineering and technology. A comprehensive review of preliminary work has been given in [5]. There are also some good reviews on the vibration of composite shell, which can be found in the literature [6–9]. Loy et al. [10] analyzed the frequency spectrum of simply supported boundary condition FGM cylindrical shells composed of stainless steel and nickel. They arrived at this fact: the frequency characteristics of FGM shells are similar to those observed in the case of homogeneous isotropic shells, and are altered by constituent volume fractions and configurations of the constituent material. Pradhan et al. [11] studied vibration characteristics of an FGM cylindrical shell made up of stainless steel and zirconia, having various boundary conditions. This analysis is performed, using beam functions and applying the Rayleigh–Ritz variational approach. In that study, the effects of boundary condition and volume fraction on shell frequencies are studied. Naeem [12] employed a polynomial based Rayleigh–Ritz approach to investigate the natural frequencies of FGM cylindrical shells under various boundary conditions. In their analysis, equations are formulated based upon Sanders' thin shell theory. Patel et al. [13]

* Corresponding author.
E-mail address: rahimi_gh@modares.ac.ir (G.H. Rahimi).

1026-3098 © 2012 Sharif University of Technology. Production and hosting by Elsevier B.V. Open access under CC BY-NC-ND license.
Peer review under responsibility of Sharif University of Technology.

doi:10.1016/j.scient.2011.11.026

Production and hosting by Elsevier
ELSEVIER

analyzed the problem of the free vibration of FGM elliptical cylindrical shells, using the Finite Element Method (FEM), based on the Higher order Shear Deformation Theory (HSDT). Based on the First order Shear Deformation Theory (FSDT), Ansari and Darvizeh [14] proposed a novel unified exact approach to investigate the vibrational behavior of FGM shells under arbitrary boundary conditions. Also, there are several studies on determining the vibration frequencies of FGM shells that can be found in the literature [15,16].

Work on the free vibration of cylindrical shells with ring supports is rare. Until now, most investigations carried out on the vibration of ring supported cylindrical shells have been restricted to isotropic shells [17–21], and no work on the vibration of ring supported FGM cylindrical shells has been seen in the literature, to the best of the authors' knowledge.

The present paper deals with the free vibration of FGM shells with arbitrarily placed ring supports along the axial direction, based on Sanders' shell theory. The displacement fields considered consist of beam eigenfunctions, which guarantee the satisfaction of edge boundary conditions, trigonometric and polynomial functions, in order to preserve periodicity in the hoop direction and zero lateral deflection at the ring supports, respectively. The aim of this investigation is to propose a simpler, but still accurate, method, capable of predicting the natural frequencies of ring supported FGM cylindrical shells under various boundary conditions. The influence of some commonly used boundary conditions, changes in ring support position and variations of shell geometrical parameters on vibration characteristics are studied.

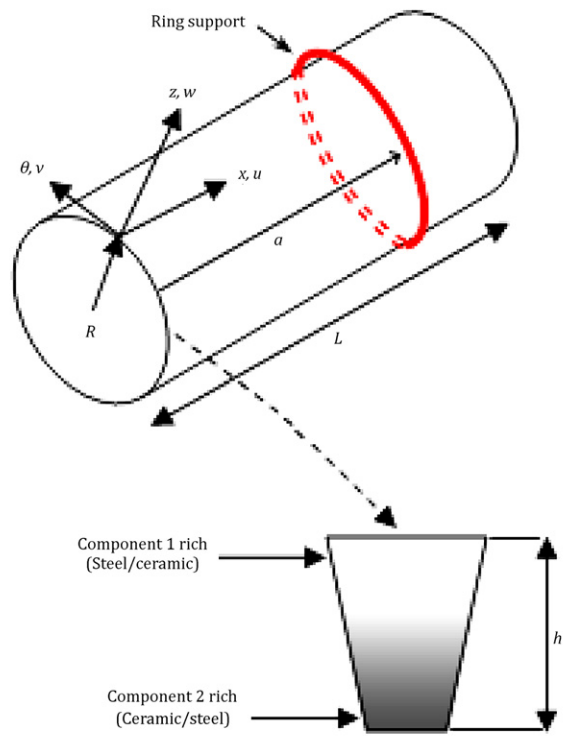

Figure 1: An element of a FGM shell with an intermediate ring support.

2. Theoretical formulation

Consider a cylindrical shell made of FGM, with internal ring support whose cross-sectional view is shown in Figure 1. Its geometrical parameters are described by R, the radius of the shell middle surface, h, the thickness of the shell and a, the position of the ring support along the axial direction of the cylindrical shell. u, v and w are deformations in the x, θ and z directions, respectively.

Assuming a plane stress condition, the constitutive relation for a thin cylindrical shell can be written by the two-dimensional Hooke's law as:

$$\begin{Bmatrix}\sigma_x\\ \sigma_\theta\\ \sigma_{x\theta}\end{Bmatrix}=\begin{bmatrix}Q_{11} & Q_{12} & 0\\ Q_{12} & Q_{22} & 0\\ 0 & 0 & Q_{66}\end{bmatrix}\begin{Bmatrix}e_x\\ e_\theta\\ e_{x\theta}\end{Bmatrix}, \tag{1}$$

where $\{\sigma\}$ is the stress vector, $\{e\}$ is the strain vector and Q_{ij}, denotes the plane stress-reduced stiffness, which, for a FGM cylindrical shell, can be defined as:

$$\begin{aligned}Q_{11}&=Q_{22}=\frac{E(z)}{1-\upsilon(z)^2}\\ Q_{12}&=\frac{\upsilon(z)E(z)}{1-\upsilon(z)^2}\\ Q_{66}&=\frac{E(z)}{2(1+\upsilon(z))}.\end{aligned} \tag{2}$$

Here, $E(z)$ and $\upsilon(z)$ are the Young's modulus and Poisson's ratio variations in the thickness direction, and will be defined later.

Based on the Sanders' thin shell theory [22], the strain components at any point of the thickness can be written as linear functions of the thickness co-ordinate, z, and the surface strains and curvatures as:

$$\begin{aligned}e_x&=\varepsilon_x-zK_x,\\ e_\theta&=\varepsilon_\theta-zK_\theta,\\ e_{x\theta}&=\gamma_{x\theta}-zK_{x\theta}.\end{aligned} \tag{3}$$

The force and moment resultants are defined as:

$$\begin{aligned}\{N_x,N_\theta,N_{x\theta}\}&=\int_{-h/2}^{h/2}\{\sigma_x,\sigma_\theta,\sigma_{x\theta}\}\mathrm{d}z,\\ \{M_x,M_\theta,M_{x\theta}\}&=\int_{-h/2}^{h/2}\{\sigma_x,\sigma_\theta,\sigma_{x\theta}\}z\mathrm{d}z.\end{aligned} \tag{4}$$

Using Eqs. (1) and (3), the relationships between boundary forces and surface strains and curvatures for a cylindrical shell are given as:

$$\begin{Bmatrix}N_x\\ N_\theta\\ N_{x\theta}\\ M_x\\ M_\theta\\ M_{x\theta}\end{Bmatrix}=\begin{bmatrix}A_{11} & A_{12} & 0 & B_{11} & B_{12} & 0\\ A_{12} & A_{22} & 0 & B_{12} & B_{22} & 0\\ 0 & 0 & A_{66} & 0 & 0 & B_{66}\\ B_{11} & B_{12} & 0 & D_{11} & D_{12} & 0\\ B_{12} & B_{22} & 0 & D_{12} & D_{22} & 0\\ 0 & 0 & B_{66} & 0 & 0 & D_{66}\end{bmatrix}\begin{Bmatrix}\varepsilon_x\\ \varepsilon_\theta\\ \gamma_{x\theta}\\ K_x\\ K_\theta\\ K_{x\theta}\end{Bmatrix}, \tag{5}$$

where A_{ij}, B_{ij} and D_{ij} are the stiffness of the FGM shell as:

$$(A_{ij},B_{ij},D_{ij})=\int_{-h/2}^{h/2}Q_{ij}(1,z,z^2)\mathrm{d}z, \tag{6}$$

and:

$$\begin{aligned}\varepsilon_x&=u_{,x},\\ \varepsilon_\theta&=\frac{1}{R}(v_{,\theta}+w),\\ \gamma_{x\theta}&=\frac{1}{R}u_{,\theta},\\ K_x&=w_{,xx},\\ K_\theta&=\frac{1}{R^2}(w_{,\theta\theta}-v_{,\theta}),\\ K_{x\theta}&=\frac{2}{R}\left(w_{,x\theta}+\frac{1}{4R}u_{,\theta}-\frac{3}{4}v_{,x}\right),\end{aligned} \tag{7}$$

in which the subscripts $,x$; $,xx$; $,\theta$; $,\theta\theta$; $,x\theta$, denote the partial derivatives with respect to these parameters.

Table 1: Values of β_i, λ_m and ξ_m for SNA–SNA, C–C, C–F and C–SNA boundary conditions.

Boundary configuration	Boundary conditions on ϕ	β_i $(i = 1, 2, 3, 4)$	Values for λ_m	ξ_m
SNA–SNA	$\phi(0) = \phi''(0) = 0$, $\phi(L) = \phi''(L) = 0$	$\beta_1 = \beta_2 = 0$, $\beta_3 = 0,\ \beta_4 = -1$	$m\pi$	1
C–C	$\phi(0) = \phi'(0) = 0$, $\phi(L) = \phi'(L) = 0$	$\beta_1 = \beta_3 = 1$, $\beta_2 = \beta_4 = -1$	$\cos\lambda_m \cosh\lambda_m = 1$	$\frac{\cosh\lambda_m - \cos\lambda_m}{\sinh\lambda_m - \sin\lambda_m}$
C–F	$\phi(0) = \phi'(0) = 0$, $\phi''(L) = \phi'''(L) = 0$	$\beta_1 = \beta_3 = 1$, $\beta_2 = \beta_4 = -1$	$\cos\lambda_m \cosh\lambda_m = -1$	$\frac{\sinh\lambda_m - \sin\lambda_m}{\cosh\lambda_m + \cos\lambda_m}$
C–SNA	$\phi(0) = \phi'(0) = 0$, $\phi(L) = \phi''(L) = 0$	$\beta_1 = \beta_3 = 1$, $\beta_2 = \beta_4 = -1$	$\tan\lambda_m = \tanh\lambda_m$	$\frac{\cosh\lambda_m - \cos\lambda_m}{\sinh\lambda_m - \sin\lambda_m}$

3. Functionally graded shells

Consider an FGM shell made of a mixture of ceramic and metal. The material properties vary continuously across the thickness, based on the following relations:

$$\begin{aligned} E(z) &= E_m + E_{cm}V_f(z), \quad E_{cm} = E_c - E_m, \\ \nu(z) &= \nu_m + \nu_{cm}V_f(z), \quad \nu_{cm} = \nu_c - \nu_m, \\ \rho(z) &= \rho_m + \rho_{cm}V_f(z), \quad \rho_{cm} = \rho_c - \rho_m \end{aligned} \tag{8}$$

where subscripts, m and c, refer to the metal and ceramic properties, respectively, $V_f(z)$ denote the volume fraction of the constituents, which, for a power-law FGM, can be defined by the following function [23,24]:

$$V_f(z) = \left(\frac{z}{h} + \frac{1}{2}\right)^N, \tag{9}$$

where N is the material index, which indicates the material variation profile through the shell thickness. For further details, the reader is referred to [14]. As can be seen, $N = 0$ and $N = \infty$ refer to isotropic shells made of ceramic and metal, respectively.

4. Strain and kinetic energy of the shell

The strain and kinetic energy of a cylindrical shell can be defined as:

$$\begin{aligned} U &= \frac{1}{2}\iiint \{e\}^T\{\sigma\}\mathrm{d}V, \\ T &= \frac{1}{2}\iiint \rho(\dot{u}^2 + \dot{v}^2 + \dot{w}^2)\mathrm{d}V, \end{aligned} \tag{10}$$

where ρ is the mass density. Substituting from Eq. (1) and integrating in the thickness direction, the strain and kinetic energies can be obtained as:

$$\begin{aligned} U &= \frac{1}{2}\iint \{\varepsilon\}^T[S]\{\varepsilon\}\mathrm{d}A, \\ T &= \frac{1}{2}\iint \rho_h(\dot{u}^2 + \dot{v}^2 + \dot{w}^2)\mathrm{d}A, \end{aligned} \tag{11}$$

where ρ_h is the density per unit length, and can be obtained as:

$$\rho_h = \int_{-h/2}^{h/2} \rho\mathrm{d}z, \tag{12}$$

and:

$$[S] = \begin{bmatrix} A & B \\ B & D \end{bmatrix},$$

is the stiffness matrix, with A_{ij}, B_{ij} and D_{ij} defined as in Eq. (6).

For a circular cylindrical shell, with an arbitrary number of ring supports, the displacement field can be written in the following form for any circumferential wave number n [17]:

$$\begin{aligned} u(x,\theta,t) &= A\frac{\partial\phi(x)}{\partial x}\cos(n\theta)\cos(\omega t), \\ v(x,\theta,t) &= B\phi(x)\sin(n\theta)\cos(\omega t), \\ w(x,\theta,t) &= C\phi(x)\prod_{i=1}^{N_r}(x - a_i)^{\zeta_i}\cos(n\theta)\cos(\omega t). \end{aligned} \tag{13}$$

In Eq. (13), A, B and C denote the amplitudes of vibrations in the x, θ and z directions, $\phi(x)$ is the axial function that satisfies the geometric boundary conditions [17], a_i is the axial position of the ith ring support, N_r stands for the number of ring supports, ζ_i is a parameter having a value of 1 if a ring support exists and 0 value if there is no ring support, and ω is the natural angular frequency of the vibration. From the assumed displacement fields in Eq. (13), only the transverse displacement is restrained on a ring support.

The axial function, $\phi(x)$, is chosen as the beam function as:

$$\begin{aligned} \phi(x) = {}& \beta_1\cosh\left(\frac{\lambda_m x}{L}\right) + \beta_2\cos\left(\frac{\lambda_m x}{L}\right) \\ & - \xi_m\left(\beta_3\sinh\left(\frac{\lambda_m x}{L}\right) + \beta_4\sin\left(\frac{\lambda_m x}{L}\right)\right), \end{aligned} \tag{14}$$

where β_i $(i = 1, 2, 3, 4)$ are some constants which depend on the boundary conditions of the cylindrical shell. The boundary conditions considered in this study are simply supported–simply supported (SNA–SNA), Clamped–Clamped (C–C), Clamped–Free (C–F) and clamped–simply supported (C–SNA). The end configurations, values of β_i, λ_m and ξ_m for these end conditions are listed in Table 1.

5. Frequency equations for FGM cylindrical shells with ring supports

Finally, the energy functional is given by the following Lagrangian function:

$$\prod = T_{\max} - U_{\max}. \tag{15}$$

The governing equations of motion for the free vibrations of ring supported FGM cylindrical shells can be derived by minimizing the above energy functional, with respect to the unknown coefficients, as follows:

$$\frac{\partial\prod}{\partial A} = \frac{\partial\prod}{\partial B} = \frac{\partial\prod}{\partial C} = 0. \tag{16}$$

Table 2: Mechanical properties of constituent materials for FGM shells.

	Stainless steel		Zirconia	
	E (N m^{-2})	υ	E (Nm^{-2})	υ
P_{-1}	0	0	0	0
P_0	201.04E9	0.3262	244.27E9	0.28
P_1	3.08E−4	−2E−4	−1.37E−3	1.13E−4
P_2	−6.53E−7	3.8E−7	1.21E−6	0
P_3	0	0	−3.68E−10	0
ρ	8166 (kg m^{-3})		5700 (kg m^{-3})	

Table 3: Comparison of frequency parameter, $\Omega = \omega R\sqrt{(1-\upsilon^2)\rho/E}$, for a clamped–clamped isotropic cylindrical shell ($m = 1,\ \upsilon = 0.3$).

n	Shell parameters		Chung [26]	Present
	L/R	R/h		
2	10	20	0.05784	0.05921
3	2	20	0.3118	0.3259
4	10	500	0.01508	0.01547

Therefore, the three governing eigenvalue equations can be obtained in the matrix form as:

$$\begin{bmatrix} C_{11} & C_{12} & C_{13} \\ & C_{22} & C_{23} \\ \text{Symm.} & & C_{33} \end{bmatrix} \begin{bmatrix} A \\ B \\ C \end{bmatrix} = 0. \tag{17}$$

For a nontrivial solution of Eq. (17), the determinant of the coefficient matrix must vanish;

$$|C_{ij}| = 0 \quad (i, j = 1, 2, 3), \tag{18}$$

resulting in a characteristic equation which is a polynomial in even powers of ω as:

$$\alpha_3\omega^6 + a_2\omega^4 + \alpha_1\omega^2 + \alpha_0 = 0, \tag{19}$$

whose eigenvalues are the natural frequencies of the ring supported FGM cylindrical shell. The corresponding eigenvectors also determine the mode shapes.

6. Material properties of FGM

Since most FGMs are used in high temperature environments, the dependency of their mechanical properties on temperature should be considered. A typical material property, P_i, which is a function of the temperature, is given as [25]:

$$P_i = P_0(P_{-1}T^{-1} + 1 + P_1T + P_2T^2 + P_3T^3), \tag{20}$$

in which P_{-1} to P_3 are unique constants of each constituent material. The constituent materials considered here are stainless steel and zirconia with properties listed in Table 2 [11].

7. Results and discussion

In order to validate the analysis proposed herein, the frequency parameter $\Omega = \omega R\sqrt{((1-\upsilon^2)\rho/E)}$ of a C–C isotropic cylindrical shell without any ring support is listed in Table 3 in comparison with that obtained by Chung [26]. Tables 4 and 5 show comparisons of the natural frequencies obtained here with those of Chung [26] and Warburton [27] for C–F and SNA–SNA isotropic cylindrical shells, respectively. From the comparisons made here, it can be clearly seen that the results of the present analysis agree well with those in the literature. Figure 2 illustrates the influence of boundary conditions on the natural frequencies of an FGM shell at room temperature, without ring supports. The obtained results are compared with those reported in [14], which show excellent agreement. The power-law exponent, N, of the FGM material is considered to have a value of 10, and the ratio, h/R, is taken as 0.002, hereafter. As expected before, the double clamped composite shell has the highest natural frequencies among selected boundary conditions. This is mainly due to the fact that the stiffness of a cylindrical shell with all edges clamped is higher than that of a shell with all edges SNA. Moreover, frequency curves converge for circumferential wave numbers greater than four, i.e. the effects of boundary conditions are only prominent for low circumferential mode numbers. Figure 3 illustrates the variation of the natural frequency with the circumferential wave number, n, for an FGM cylindrical shell with a ring support at $a = 0.3L$ and subjected to different boundary conditions. As shown in this figure, the frequencies for four mentioned boundary conditions increased with an increment in circumferential wave number. This increase is significant when n increased from 1 to 2, and for greater values of n, the frequencies increased gradually. It should be mentioned that this figure is similar to that obtained for isotropic cylindrical shells in [17]. Figure 4 shows a variation of the fundamental natural frequency versus the position of the ring support for SNA–SNA, C–C and C–F boundary conditions. As shown in this figure, for symmetric boundary conditions, such as SNA–SNA and C–C boundary conditions, the fundamental frequency curve is symmetrical about the center of the shell. This means that for symmetric boundary conditions, the maximum fundamental frequency is achieved when the ring support is in the middle of the cylindrical shell. But, for asymmetric end conditions, such as C–F, the frequency curve is not symmetrical about the center of the shell as expected. It should be pointed that this figure is very similar to the one plotted in the case of isotropic cylindrical shells [17]. Figures 5–7 clarify the variation of the fundamental natural frequency of the FGM cylindrical shell against the position of the ring support at different L/R ratios for SNA–SNA, C–C and C–F end conditions. As can be observed, the frequencies are **higher** at large L/R ratios. Also, the influence of the ring support position is prominent at large L/R ratios. Table 6 presents a comparison between the fundamental natural frequencies of an FGM shell with and without ring supports. As can be observed, the natural frequencies of a shell with ring support are higher than those of a shell without any support, and the difference between these values is significant. The nomenclature of an FGM cylindrical shell with two internal ring supports is shown in Figure 8. Figures 9–11 represent the variations of the natural frequencies with the positions of the two ring supports for SNA–SNA, C–C and C–F FGM cylindrical shells, respectively. The two internal ring supports are assumed to be placed at equal intervals from the two ends ($a_1/L = X$, $a_2/L = 1 - X$). These figures illustrate that for three mentioned boundary conditions, the natural frequencies are the lowest when the two rings are at the two ends of the shell. As the two ring supports approach each other, the frequencies increase and then decrease. For example, in the case of SNA–SNA and C–C cylindrical shells, the maximum value of the natural frequency occurs when x is in the range 0.32–0.36. While for C–F boundary conditions, this range is read as 0.14–0.18. A comparison between the frequency variation of SNA–SNA and C–C FGM shells versus the positions of two ring supports is graphically illustrated in Figure 12 ($n = 1$). It is found that the frequencies of SNA–SNA shells are higher than that of C–C ones, when the two rings are near the ends. However, by approaching the rings towards the

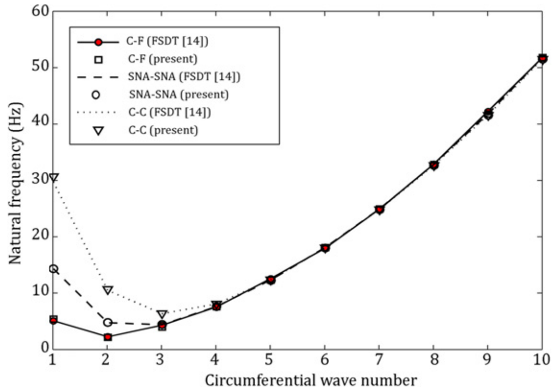

Figure 2: Frequency variation associated with different boundary conditions for a FGM shell without ring supports ($m = 1, L/R = 20$).

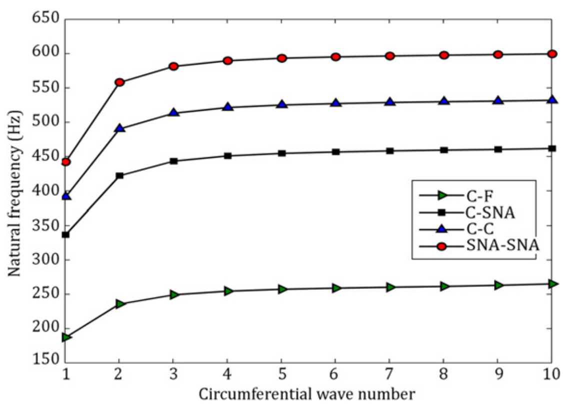

Figure 3: Variation of the natural frequencies with the circumferential wave number for an FGM cylindrical shell with a ring support and various boundary conditions ($m = 1, L/R = 20, a/L = 0.3$).

Table 4: Comparison of natural frequencies (Hz) for a clamped–free isotropic cylindrical shell ($L = 51.12$ cm, $R = 21.62$ cm, $h = 0.15$ cm, $E = 183$ GPa, $\rho = 7492$ kg/m^3, $\upsilon = 0.3$).			
m	n	Chung [26]	Present
1	2	403.72	452.12
	3	223.34	240.92
	4	171.77	180.03
	5	199.16	204.94
	6	268.86	275.19
	7	361.92	369.97
	8	472.54	482.87
	9	599.03	612.03

center of the shell, the natural frequencies related to the C–C boundary condition exceed those of the SNA–SNA counterpart. As a reason for this, when both ring supports are at the vicinity of shell ends, the influence of the ring supports are dominant, compared to that of end supports. Figure 13 represents the normalized displacement, w^*, $w^* = w/w_{\max}$ where $w_{\max}$ is the absolute maximum displacement along the x direction for a FGM cylindrical shell with one ring support placed at 0.2L from the left end. Figure 14 shows the similar mode shape for an FGM cylindrical shell with two ring supports placed at 0.2L and 0.8L from the left end. The satisfaction of the geometrical boundary conditions at the ring supports can be readily seen as well.

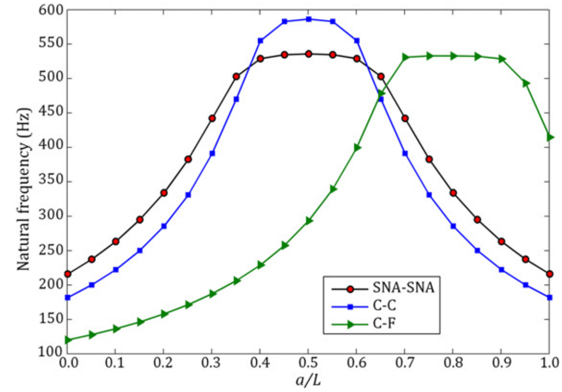

Figure 4: Variation of the fundamental natural frequency with the position of the ring support a/L for SNA–SNA, C–C and C–F FGM cylindrical shell ($m = 1$, $n = 1$, $L/R = 20$).

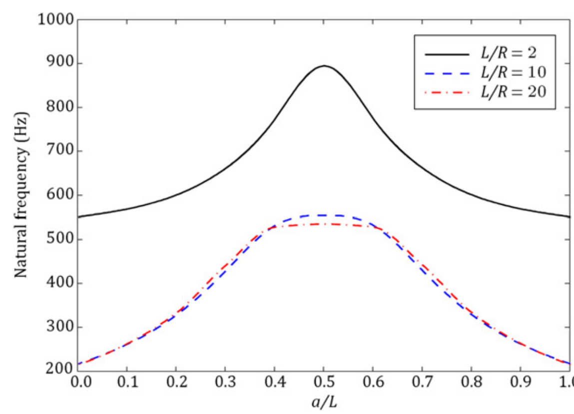

Figure 5: Variation of the fundamental frequency with the position of the ring support at different L/R ratios for SNA–SNA boundary condition ($m = 1, n = 1$).

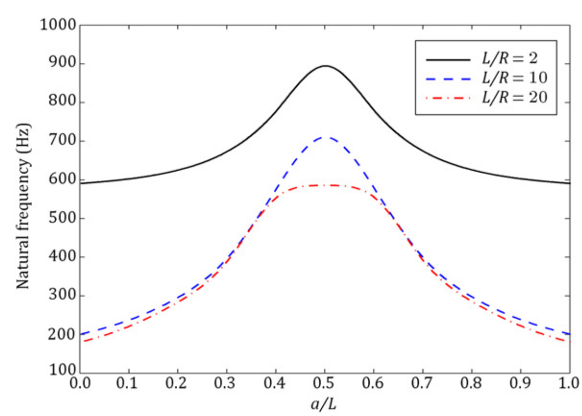

Figure 6: Variation of the fundamental frequency with the position of the ring support at different L/R ratios for C–C boundary condition ($m = 1, n = 1$).

8. Conclusion

A study has been presented to investigate the vibrational behavior of power-law FGM cylindrical shells with intermediate ring supports placed along the length, and new exact vibration frequencies were reported. Theoretical formulations were carried out, based on Sanders' thin shell theory, in which the governing equations of motion were derived using energy functional and the Ritz technique. The influence of some commonly

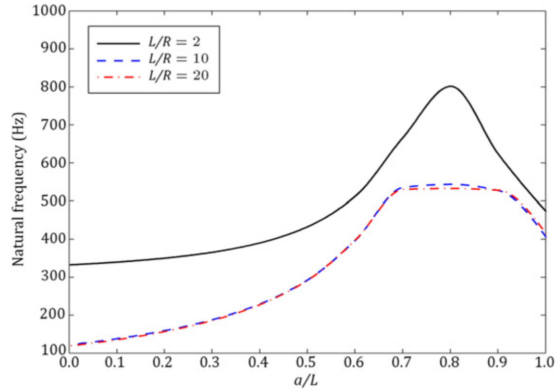

Figure 7: Variation of the fundamental frequency with the position of the ring support at different L/R ratios for C–F boundary condition ($m = 1, n = 1$).

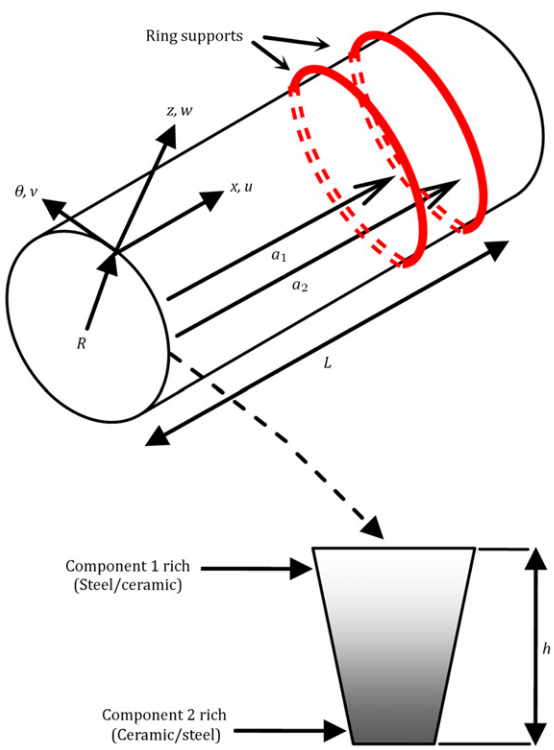

Figure 8: FGM shell with two intermediate ring supports.

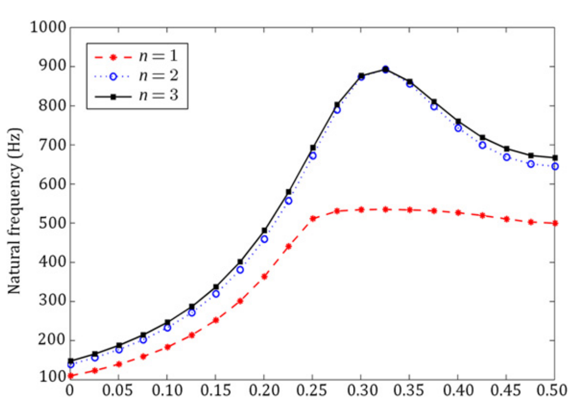

Figure 9: Variation of the natural frequency with the circumferential wave number at different positions of two ring supports for a SNA–SNA FGM cylindrical shell ($m = 1, L/R = 20$).

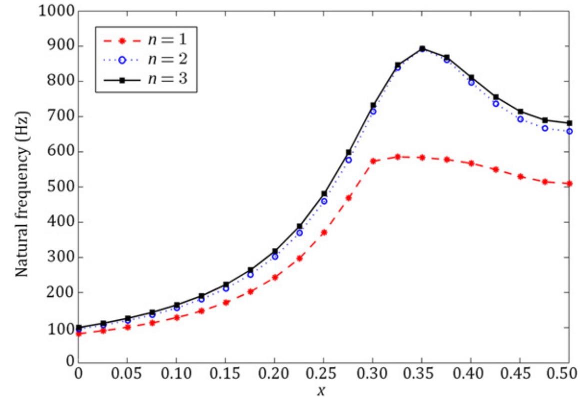

Figure 10: Variation of the natural frequency with the circumferential wave number at different positions of two ring supports for a C–C FGM cylindrical shell ($m = 1, L/R = 20$).

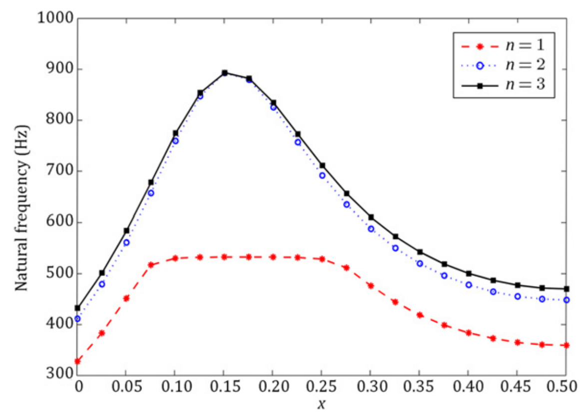

Figure 11: Variation of the natural frequency with the circumferential wave number at different positions of two ring supports for a C–F FGM cylindrical shell ($m = 1, L/R = 20$).

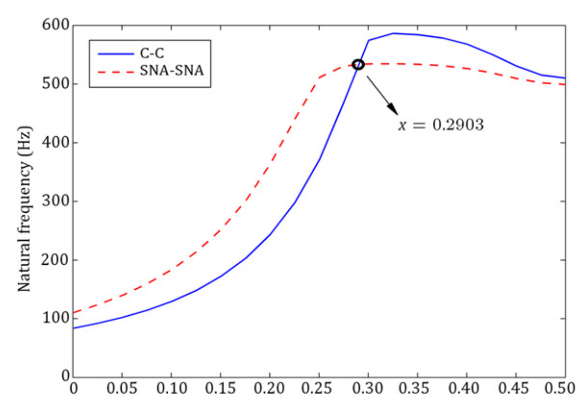

Figure 12: Variation of the natural frequency against the position of two ring supports for an FGM cylindrical shell with different boundary conditions ($m = 1, L/R = 20$).

used boundary conditions, the effect of changes in shell geometrical parameters and variations of ring support position on vibration characteristics are discussed. The obtained results for some special cases show excellent agreement with those available in the literature. For symmetric boundary conditions, such as SNA–SNA and C–C, the fundamental frequency decreased as the ring support travelled from the center towards either end of the shell. However, for shells with asymmetric end conditions,

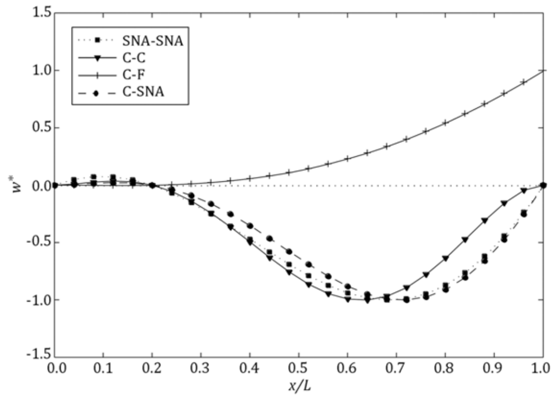

Figure 13: Normalized displacement w^* along the x direction for a FGM shell with one ring support under various boundary conditions ($m = 1$, $n = 1$, $L/R = 20$, $a/L = 0.2$, $q = 30°$, $t = 5$ s).

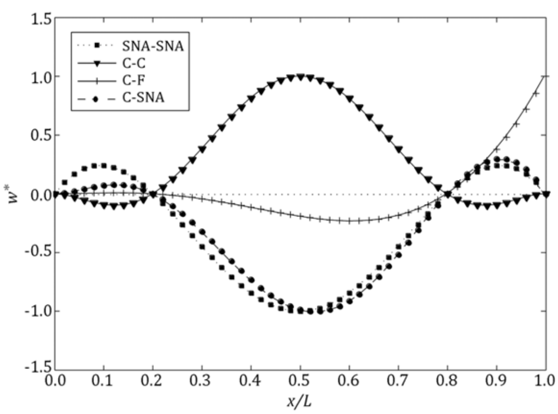

Figure 14: Normalized displacement w^* along the x direction for a FGM shell with two ring supports under various boundary conditions ($m = 1$, $n = 1$, $L/R = 20$, $a_1/L = 0.2$, $a_2/L = 0.8$, $q = 30°$, $t = 5$ s).

Table 5: Comparison of natural frequencies (Hz) for a simply supported–simply supported isotropic cylindrical shell ($L = 8$ in., $R = 2$ in., $h = 0.1$ in., $E = 30 \times 10^6$ lbf/in.^{2}, $\upsilon = 0.3$, $\rho = 7.35 \times 10^{-4}$ lbfs^2/in.^{4}).

n	m	Warburton [27]	Present
2	1	2,046.8	2,043.7
	2	5,637.6	5,635.4
	3	8,935.3	8,932.5
	4	11,405	11,407.5
	5	13,245	13,253.2
3	1	2,199.3	2,195.1
	2	4,041.9	4,035.5
	3	6,620.0	6,614.6
	4	9,124.0	9,121.0
	5	11,357	11,359.0

Table 6: Comparison of natural frequencies (Hz) for an FGM shell with and without ring support ($m = 1$, $n = 1$).

	a/L	Boundary conditions	
		SNA–SNA	C–F
With ring support	0	216.8235	120.8547
	0.2	334.7145	158.7590
	0.5	536.5472	294.2014
	0.8	334.7145	533.7894
	1	216.8235	415.6396
Without ring support		14.4260	5.4853

like C–F, it is seen that the optimal ring support location to maximize the natural frequency shifts away from the shell centre and lies in the range $a/L = 0.6$–0.9.

In the absence of ring supports, as one travels through the end conditions of SNA–SNA to fully clamped, denoted by C–C, respectively, the influence of boundary conditions is shown to increase natural frequencies. When the ring supports are placed at the vicinity of shell ends, the effects of ring supports are dominant, compared to that of end supports, and this results in higher frequency values for SNA–SNA shells. However, by approaching the ring supports towards the center of the shell, the trend becomes reversed.

Another point deduced here is that for a shell with two rings, the lowest frequency of the shell with any type of boundary condition occurs when the two rings are at two ends of the shell. Also, in SNA–SNA and C–C cylindrical shells, the maximum value of the natural frequency occurs when the position of one of the rings over the length of the cylinder lies in the range 0.32–0.36, while for C–F boundary conditions, this range is read as 0.14–0.18. The present analysis is a promising approach and can be readily implemented for obtaining the natural frequencies of a FGM shell corresponding to axial mode numbers higher than one ($m > 1$).

References

[1] Yamanouchi, M., Koizumi, M., Hirai, T. and Shiota, I. *Proceedings of the First International Symposium on Functionally Gradient Materials* (1990).
[2] Koizumi, M. "The concept of FGM, ceramic transactions", *Functionally Gradient Materials*, 34, pp. 3–10 (1993).
[3] Miyamoto, Y., Kaysser, W.A., Rabin, B.H., Kawasaki, A. and Ford, R.G., *Functionally Graded Materials: Design, Processing and Applications*, Kluwer Academic Publishers, London (1999).
[4] Moya, J.S. "Layered ceramics", *Advanced Materials*, 7, pp. 185–189 (1995).
[5] Leissa, A.W. "Vibration of shells", NASA SP-288 US Govt. Printing Office, 1973.
[6] Vanderpool, M.E.V. and Bert, C.W. "Vibration of materially monoclinic, thick-wall circular cylindrical shells", *AIAA Journal*, 19, pp. 634–641 (1981).
[7] Lan, K.Y. and Loy, C.T. "Influence of boundary conditions and fiber orientation and the natural frequencies of thin orthotropic laminated cylindrical shells", *Composite Structures*, 31, pp. 21–30 (1995).
[8] Sharma, C.B., Darvizeh, M. and Darvizeh, A. "Natural frequency response of vertical cantilever composite shells containing fluid", *Engineering Structures*, 20(8), pp. 732–737 (1998).
[9] Sharma, C.B., Darvizeh, M. and Darvizeh, A. "Free vibration behaviour of helically wound cylindrical shells", *Composite Structures*, 44, pp. 55–62 (1999).
[10] Loy, C.T., Lam, K.Y. and Reddy, J.N. "Vibration of functionally graded cylindrical shells", *International Journal of Mechanica. Sciences*, 41, pp. 309–324 (1999).
[11] Pradhan, S.C., Loy, C.T., Lam, K.Y. and Reddy, J.N. "Vibration characteristics of functionally graded cylindrical shells under various boundary conditions", *Applied Acoustics*, 61, pp. 111–129 (2000).
[12] Naeem, M.N. "Prediction of natural frequencies for functionally graded cylindrical shells", Ph.D. Thesis, UMIST, UK (2004).
[13] Patel, B.P., Gupta, S.S., Loknath, M.S. and Kadu, C.P. "Free vibration analysis of functionally graded elliptical cylindrical shells using higher order theory", *Composite Structures*, 69, pp. 259–270 (2005).
[14] Ansari, R. and Darvizeh, M. "Prediction of dynamic behaviour of FGM shells under arbitrary boundary conditions", *Composite Structures*, 85(4), pp. 284–292 (2008).
[15] Tornabene, F., Viola, E. and Inman, D.J. "2-D differential quadrature solution for vibration analysis of functionally graded conical, cylindrical shell and annular plate structures", *Journal of Sound and Vibration*, 328, pp. 259–290 (2009).
[16] Li, S.R., Fu, X.H. and Batra, R.C. "Free vibration of three-layer circular cylindrical shells with functionally graded middle layer", *Mechanics Research Communications*, 37, pp. 577–580 (2010).
[17] Loy, C.T. and Lam, K.Y. "Vibration of cylindrical shells with ring support", *International Journal of Mechanical Sciences*, 39(4), pp. 445–471 (1997).
[18] Xiang, Y., Ma, Y.F., Kitipornchai, S., Lim, C.W. and Lau, C.W.H. "Exact solutions for vibration of cylindrical shells with intermediate ring supports", *International Journal of Mechanical Sciences*, 44, pp. 1907–1924 (2002).
[19] Zhang, L. and Xiang, Y. "Vibration of open circular cylindrical shells with intermediate ring supports", *International Journal of Solids and Structures*, 43, pp. 3705–3722 (2006).

[20] Jafari, A.A. and Bagheri, M. ''Free vibration of non-uniformly ring stiffened cylindrical shells using analytical, experimental and numerical methods'', *Thin-Walled Structures*, 44, pp. 82–90 (2006).
[21] Pan, Z., Li, X. and Ma, J. ''A study on free vibration of a ring-stiffened thin circular cylindrical shell with arbitrary boundary conditions'', *Journal of Sound and Vibration*, 314, pp. 330–342 (2008).
[22] Sanders, J.L. ''An improved first approximation theory for thin shells'', NASA Report NASA-TR-24, 1959.
[23] Chi, S.H. and Chung, Y.L. ''Mechanical behavior of functionally graded material plates under transverse load — part I: analysis'', *International Journal of Solids and Structures*, 43, pp. 3657–3674 (2006).
[24] Chi, S.H. and Chung, Y.L. ''Mechanical behavior of functionally graded material plates under transverse load — part II: numerical results'', *International Journal of Solids and Structures*, 43, pp. 3657–3691 (2006).
[25] Touloukian, Y.S., *Thermophysical Properties of High Temperature Solid Materials*, Macmillan, New York (1967).
[26] Chung, H. ''Free vibration analysis of circular cylindrical shells'', *Journal of Sound and Vibration*, 74(3), pp. 331–350 (1981).
[27] Warburton, G.B. ''Vibration of thin cylindrical shells'', *Journal of Mechanical Engineering Science*, 7, pp. 399–407 (1965).

Gholam Hossein Rahimi received his Ph.D. from UMIST, England, in 1990, and is now Associate Professor. His research interests include computational solid mechanics, design, manufacture and test of grid composite structures, and analysis of FG and FGP solid structures. His specialty areas are continuum mechanics, finite element, elasticity and analysis of plates and shells. Professor Rahimi has published more than 40 research papers in national and international journals, and more that 50 papers have been presented at national and international conferences.

Reza Ansari received his Ph.D. from the University of Guilan, Iran, in 2008, and was also a visiting fellow at Wollongong University, Australia, from 2006 to 2007. He is currently Assistant Professor and faculty member of the Department of Mechanical Engineering at the University of Guilan. He has authored more than 40 journal papers and 12 book chapters. His research background and interests include computational nanomechanics, advanced numerical techniques, nonlinear analyses, and prediction of the mechanical behavior of smart composite/FGM shell-type structures.

Milad Hemmatnezhad was born in Iran, in 1986. He received the B.S. and M.S. Degrees in Mechanical Engineering from the University of Guilan in Rasht, Iran, in 2006 and 2009, respectively. He has published several research papers in various fields, such as the vibration of composite and FGM cylindrical shells, application of perturbation methods for solving nonlinear differential equations, nonlinear oscillations of multiwalled carbon nanotubes, etc. In September 2010, he joined Tarbiat Modares University of Tehran, Iran, to pursue a Ph.D. Degree in Mechanical Engineering.